A&A 539, A14 (2012)
DOI: 10.1051/0004-6361/201116934

Astronomy & Astrophysics

Planetary transit candidates in the CoRoT-SRc01 field⋆,⋆⋆,⋆⋆⋆

A. Erikson[1], A. Santerne[2], S. Renner[1,3,4], P. Barge[2], S. Aigrain[5], A. Alapini[6], J.-M. Almenara[7,25,2], R. Alonso[8], M. Auvergne[9], A. Baglin[9], W. Benz[10], A. S. Bonomo[2], P. Bordé[11], F. Bouchy[12,13], H. Bruntt[9], J. Cabrera[1,14], L. Carone[15], S. Carpano[16], Sz. Csizmadia[1], M. Deleuil[2], H. J. Deeg[7,25], R. F. Díaz[13], R. Dvorak[17], S. Ferraz-Mello[18], M. Fridlund[16], D. Gandolfi[19,16], J.-C. Gazzano[2,20], M. Gillon[8,21], E. W. Guenther[19], T. Guillot[20], A. Hatzes[19], G. Hébrard[13], L. Jorda[2], H. Lammer[22], A. Léger[11], A. Llebaria[2], M. Mayor[8], T. Mazeh[23], C. Moutou[2], M. Ollivier[11], A. Ofir[23], M. Pätzold[15], F. Pepe[8], F. Pont[6], D. Queloz[8], M. Rabus[7,25,27], H. Rauer[1,24], C. Régulo[7,25], D. Rouan[9], B. Samuel[11], J. Schneider[14], A. Shporer[26,28,29], B. Tingley[7,25], S. Udry[8], and G. Wuchterl[19]

(Affiliations can be found after the references)

Received 21 March 2011 / Accepted 16 September 2011

ABSTRACT

Context. The space mission CoRoT is devoted to the analysis of stellar variability and the photometric detection of extrasolar planets.
Aims. We present the list of planetary transit candidates detected in the first short run observed by CoRoT that targeted SRc01, towards the Galactic center in the direction of Aquila, which lasted from April to May 2007.
Methods. Among the acquired data, we analyzed those for 1269 sources in the chromatic bands and 5705 in the monochromatic band. Instrumental noise and the stellar variability were treated with several detrending tools, to which several transit-search algorithms were subsequently applied.
Results. Fifty-one sources were classified as planetary transit candidates and 26 were followed up with ground-based observations. Until now, no planet has been detected in the CoRoT data from the SRc01 field.

Key words. techniques: photometric – techniques: radial velocities – techniques: spectroscopic – planetary systems – binaries: eclipsing

1. Introduction

The CoRoT space mission was launched in December 2006 with the dual objectives of searching for extrasolar transiting planets and a detailed characterization of stellar variability (Baglin et al. 2006). Since its launch CoRoT has been monitoring over 100 000 stars in two different regions of the sky, the *center* direction targeting the constellation of Aquila (Galactic longitude 40°), and the *anti-center* direction toward the constellation of Monoceros (Galactic longitude 210°). Owing to the orbital constraints of the satellite, target fields in these two directions can be monitored for about 150 days. These CoRoT long runs are fully devoted to stellar seismology and planet search. In addition, CoRoT short runs with a duration of around 30 days are performed in-between. Besides serving the same purpose as the long runs, these observations are also devoted to the CoRoT additional program (Weiss et al. 2004).

The mission CoRoT acquires photometric lightcurves by measuring the flux either in white light or in three colors from each target. Before being analyzed, the data are cleaned of cosmic ray hits, then corrected for spacecraft jitter and other instrumental effects. Thereafter, data access is exclusive to the CoRoT co-investigators for one year, after which it is placed in the archive of the CoRoT Data Center for general access[1]. The search for planetary transit candidates and the performed ground-based follow-up observations are summarized in this type of paper on a field-by-field basis and in a sequential order upon conclusion of the follow-up effort. The purpose is twofold. First, to make the detection yield and ground-based observational data generally available to the scientific community to allow future analysis of individual targets. Moreover, the results presented can be used to study extrasolar-planet detection statistics in general (Mayor et al. 2009; Borucki et al. 2011; Howard et al. 2011), both in comparisons to other transit surveys as well as for variations in the CoRoT fields monitored. In particular, the candidate yield in individual CoRoT fields might be correlated with the existing differences in their stellar populations.

The first results of the planetary candidate detection and confirmation of the CoRoT initial run (IRa01) and the first long run in the center direction (LRc01) were previously presented by Carpano et al. (2009), Moutou et al. (2009), Cabrera et al. (2009), respectively.

In the present paper, we report on the analysis and subsequent follow-up observations of transit candidates in the first short run in the center direction to be observed by CoRoT (SRc01 coordinates: $18^h58^m22.42^s$; 3°04′48″). The 3.05° by 2.8° field was observed for a total of 26 days between 13 April and 9 May 2007.

In the following, we describe the characteristics of the SRc01 field, the detection process to find planetary transit candidates

⋆ The CoRoT space mission, launched on December 27th 2006, has been developed and is operated by CNES, with contributions from Austria, Belgium, Brazil, ESA, Germany, and Spain. The CoRoT data are available to the community from the CoRoT archive: http://idoc-corot.ias.u-psud.fr

⋆⋆ Based in part on observations made with the 1.93-m telescope at Observatoire de Haute Provence (CNRS), France (SOPHIE Program 08A.PNP.MOUT).

⋆⋆⋆ Based in part on observations made with the ESO-3.60-m telescope at La Silla Observatory (ESO), Chile (HARPS Program ESO – 081.C-0388) and with the ESO-VLT telescope at Paranal Observatory (ESO), Chile (FLAMES Program ESO – 081.C-0413).

[1] http://idoc-corot.ias.u-psud.fr

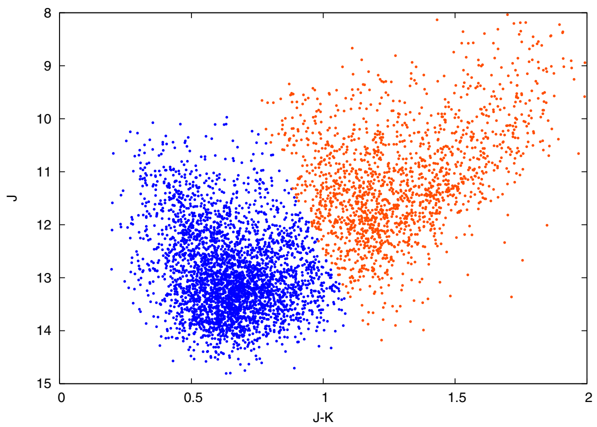

Fig. 1. $J - K$ versus J color–magnitude diagram of the 6974 stars in SRc01 field. Dwarf and giants stars are most likely to be found to the left and right, respectively.

from the CoRoT lightcurves, as well as the subsequent ground-based follow-up observations performed for a number of those candidates to determine their true character. The final yield of that process was that among the 6974 SRc01 targets observed by CoRoT, we identified 51 transit candidates and 139 eclipsing binaries. Follow-up observations were started for the candidates and a non-planetary nature has so far been established in seven cases. The remaining candidates are unresolved pending future observations.

2. Field characterization

The CoRoT SRc01 pointing was primarily chosen to cover stars within the seismology core program and has not been particularly optimized for the planet-finding programme of CoRoT. The target stars were selected using the information from ground-based surveys available in the ExoDat database (Meunier et al. 2007; Deleuil et al. 2009). Compared to CoRoT LRc01, the first long run field in the same direction of the sky (Cabrera et al. 2009), the SRc01 field contains fewer target stars and has a more inhomogeneous distribution. The number of stars observed by CoRoT is 11 408 and 6974 for the respective fields. Moreover, to increase the planet detection probability we have to consider not only the total number of stars in the field. It is equally crucial to select the field for which the fraction of dwarf stars among the target stars is optimized (Brown 2003; Batalha et al. 2010). Figure 1 shows a $J - K$ versus J color–magnitude diagram from the 2MASS survey (Skrutskie et al. 2006) for all the stars observed by CoRoT in the SRc01. Dwarfs and giants can be distinguished with the help of magnitude-limited samples in these colour-magnitude diagrams (see Deleuil et al. 2006, for its application to CoRoT data). On the basis of the division shown in the figure, the fraction of dwarf stars in the SRc01 field can be estimated to be around 65%, which is in agreement with the 68% fraction provided by the stellar classification in ExoDat (Deleuil et al. 2009). This is considerably higher than the corresponding number (42%) for the previously reported LRc01 field (Cabrera et al. 2009).

More detailed studies of the dwarf and giant populations in other CoRoT runs have appeared in the literature (Gazzano et al. 2010; Hekker et al. 2009, 2010; Miglio et al. 2009a,b; Mosser et al. 2010). The fraction of giant stars determined in previous papers are consistent with the estimates made from the color-magnitude diagrams (Aigrain et al. 2009).

3. Data acquisition and reduction

The SRc01 field was observed by CoRoT for a total of 26 days between Julian dates 2 454 193.94 and 2 454 229.81. A complete description of the satellite operations can be found in Boisnard & Auvergne (2006); Barge et al. (2008b); Auvergne et al. (2009). For the exoplanet channel of CoRoT, the light is dispersed by a bi-prism to help separate true planetary transits, which are nearly achromatic, from stellar variability. Depending on the brightness of the star, the lightcurve is either measured in chromatic mode (CHR) consisting of three separate channels (red, green, and blue), or in monochromatic mode (MON). Out of 6974 SRc01 targets, 1269 were observed in chromatic and 5705 in monochromatic mode.

During subsequent data treatment the main systematic error sources (jitter, hot pixels, outliers) are corrected or flagged (see Drummond et al. 2008; Auvergne et al. 2009; Pinheiro da Silva et al. 2008). The resulting CoRoT lightcurves are then provided for further analysis at the CoRoT N2 data level (Baudin et al. 2006). A discussion of systematic noise sources still present and how to address them, is found in Aigrain et al. (2009); Carpano et al. (2009); Cabrera et al. (2009). The data used for the analysis presented in this paper is the version 1.3 released on 1 April 2008.

4. Data analysis

The analysis of the SRc01 data set was performed by the different teams listed in Cabrera et al. (2009). All of them applied different methods for filtering and detrending the lightcurves, and searched for transit-like signals (Alapini & Aigrain 2008; Bordé et al. 2007; Carpano & Fridlund 2008; Defaÿ et al. 2001; Mazeh et al. 2009; Mislis et al. 2010; Moutou et al. 2005, 2007; Ofir et al. 2010; Régulo et al. 2007; Renner et al. 2008). The main advantage of this approach is that different methods have different types of false alarms and that a combined analysis tends to minimize their occurrence in the final candidate list (Moutou et al. 2005, 2007). In a second step the candidates found by the different teams are compared and ranked according to the quality of the signal and the planetary likelihood as described in detail in Carpano et al. (2009) and Cabrera et al. (2009); for the rate and nature of false positives, we refer to Almenara et al. (2009). The particular aim here is to identify as many as possible of the candidates for which the transit-like event can be attributed to either eclipsing binaries, contaminating binaries, or stellar activity. The outcome of this process is a ranking consisting of four separate Classes: priority 1 consists of very promising planetary candidates (see Fig. 2 for an example), priority 2 and 3 are candidates with indications of a non-planetary nature, but where there is not enough information to reject them from a pure photometric analysis, and finally priority 4 consists of candidates for which the transit signal is most likely not due to a planet. In addition, a large number of eclipsing binary systems are found during the detection process.

4.1. Detected planetary transit candidates

The 51 transit candidates found in the SRc01 field are listed in Table 10. For each case, this table indicates the priority, CoRoT identification (CoRoT-ID and CoRoT win-ID, i.e. the identification of the target window in the specific field), coordinates, B and R magnitudes from ExoDat, orbital period, epoch of the detected event, depth and length of the transit, and the outcome of ground-based follow-up observations (see Sect. 5). Table 10

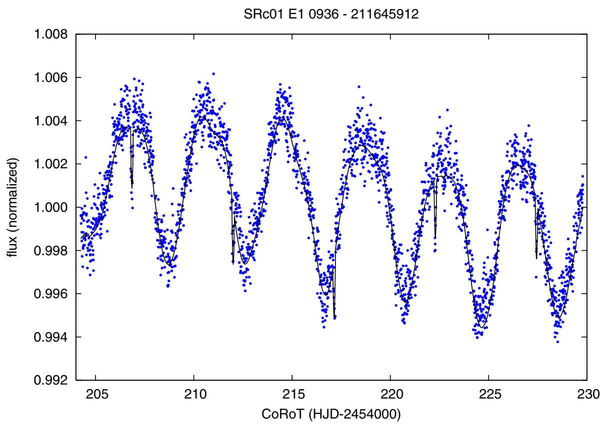

Fig. 2. Lightcurve of CoRoT SRc01 E1 0936. The variability of the star has a period of 3.93 days. Also, a transiting candidate was found with a period of 5.15 days and a depth of 0.25%.

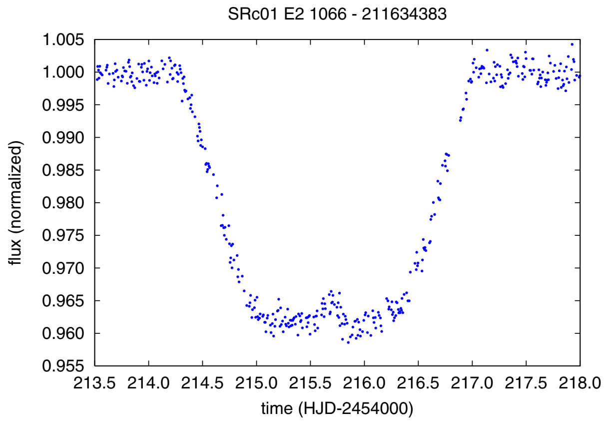

Fig. 3. The single detected transit-like event of CoRoT SRc01 E2 1066. Notable is the 0.5% local maximum at mid-transit.

indicates three priority 1 candidates, 15 priority 2 candidates, 21 priority 3 candidates, and 12 priority 4 candidates. From these, single transit events were detected for nine cases. Two of the latter are discussed below in detail.

The lightcurve of SRc01 E2 1066 (Fig. 3) shows a single event with a depth of 4% and a duration of 66h (slightly more than double the expected duration of the transit of Jupiter around the Sun). The $J-K$ color of the star (1.32) and its position in the color-magnitude diagram (Fig. 1) indicate that the target is probably a giant star, although there is no spectral confirmation that could rule out the possibility of a late dwarf star. However, from the detection point of view, the detection of this signal is similar to the challenge of detecting the transit of a Jupiter around a solar-like star with a semi-major axis of several AU. Moreover, the shape of the transit shows the characteristic signal of the passage of a transiting object across an active region of a star (see e.g. the case of TrEs-1b, Charbonneau et al. 2007; for which an alternative explanation was proposed by Rabus et al. 2009).

The lightcurve of SRc01 E1 3314 shows two events of different depth and duration. The first one occurs in HJD 2 454 211.4, and has a duration of 4.5 h and a depth of 1%; the second one is centered on HJD 2 454 216.1, and has a duration of 4.1 h and a depth of 0.7%. The $J-K$ color of the star is 0.6, which is compatible with a dwarf. There are no more events of similar amplitude in the 13 days that remained until the end of the observations. These observations are compatible with a system of two Jupiter-sized transiting planets with orbital periods longer than 13 days or with the primary and secondary eclipses of a highly eccentric eclipsing binary (as in the case of LRc01 E2 0379, Cabrera et al. 2009).

The R magnitudes of these two targets at 15.7 and 15.4, respectively, are too faint for efficient ground-based follow-up observations, which were not performed in any case.

4.2. Detected eclipsing binaries

The 139 eclipsing binaries identified in the SRc01 data set during the detection process are presented in Table 11. The CoRoT mask of SRc01 E1 1760 integrates the light of two eclipsing binaries with periods of 12.7 and 5.3 days. The field is relatively crowded and from the CoRoT measurements alone we cannot determine which of the stars in the PSF are the eclipsing binaries. This is also true for SRc01 E2 1728, which contains two binaries having periods of 1.8 and 5.3 days. SRc01 E1 3171 is probably a very eccentric binary where only one secondary eclipse was observed, although it is unclear whether the event at HJD 2 454 219.9 occurs in the same target as the primary event. The targets SRc01 E1 1827, E2 1388, E1 2373, E2 2240, E1 3240, E1 1819, E2 2115, E1 3091, E2 1418, and E1 0770 are eccentric binaries with a secondary eclipse at a phase that is different from 0.5. The star SRc01 E1 1193 (a peculiar eclipsing binary, probably with a disk), E1 2695 (with a pulsating component), E1 0836 (with giant components), and E2 1760 (classified as a delta Scuti binary by Debosscher et al. 2009) show interesting lightcurves.

More detailed analysis of individual eclipsing binary stars observed with CoRoT have been published in the literature (Damiani et al. 2010; Desmet et al. 2010; Dolez et al. 2009; Maceroni et al. 2009, 2010), but so far none of these analyses correspond to an object in this field. For an analysis of the variability of the stars in the CoRoT fields, we refer to the general works of Debosscher et al. (2009) and Sarro et al. (2009). There have also been specialized analyses of O stars (Degroote et al. 2010), B stars (Charpinet et al. 2010; Degroote et al. 2009a; Diago et al. 2009; Lefever et al. 2010; Huat et al. 2009; Neiner et al. 2009; Gutiérrez-Soto et al. 2009), solar-like stars (Appourchaux et al. 2008; Barban et al. 2009; Belkacem et al. 2009; Deheuvels et al. 2010; Deheuvels & Michel 2010; García et al. 2009, 2010; Michel et al. 2008; Mosser et al. 2009; Samadi et al. 2010), giants stars (Carrier et al. 2010; de Ridder et al. 2009), beta Cephei (Degroote et al. 2009b), delta Scuti (Poretti et al. 2009), and in particular HD 174936, observed in the asteroseismology field of SRc01 (García Hernández et al. 2009), RR Lyrae stars (Chadid et al. 2010), or HgMn stars (Alecian et al. 2009) to cite some examples.

5. Detailed follow-up of candidates

5.1. Ground based observations

The CoRoT mission has proved its ability to detect very small planets such as CoRoT-7b (Léger et al. 2009; Queloz et al. 2009), as well as planets with long orbital periods such as CoRoT-9b (Deeg et al. 2010). A ground-based follow-up observation constitutes an integrated part of the detection process, both to reject scenarios that can mimic planetary transits among the candidates found by the detection teams, as well as to confirm and characterize the CoRoT planets. Details of this process can be found in Deeg et al. (2009) for the photometric follow-up and in Moutou et al. (2009) for the spectroscopic observations.

Table 1. Instruments and methods used in the follow-up observations of the SRc01 candidates.

Instrument	Diameter	Nights	Method	Measurements	Program ID
IAC80	0.8	4	photometry	on-target transit confirmation	–
EulerCam	1.2	1	photometry	on-target transit confirmation	–
Wise	1.0	1	photometry	on-target transit confirmation	–
SOPHIE	1.93	2	radial velocity	SB identification, mass characterization	08A.PNP.MOUT
HARPS	3.6	3	radial velocity	mass characterization	ESO – 081.C-0388
FLAMES/ UVES	8.2	1	radial velocity	SB identification, mass characterization	ESO – 081.C-0413

The instruments used during the ground-based follow-up of the SRc01 transiting candidates are listed in Table 1.

5.1.1. Photometric follow-up

High-precision photometric follow-up is needed to discard contaminating eclipsing binaries located inside or in the neighborhood of the CoRoT photometric mask. The objective of such an observation is to re-observe a transit with a high spatial resolution (seeing limited) and check the flux variations of all nearby stars. We note that for photometric follow-up, a precise prediction of expected transit times is needed. Owing to the relatively short observing span of SRc01 of 26 days, the precision of candidate periods is significantly lower than those of the CoRoT long runs. This leads to a larger error in transit predictions that implying that short run candidates need to be re-observed from the ground as quickly as possible. For typical Hot-Jupiter transit candidates, ground-based transit observations become unfeasible about one year after the CoRoT-observations, when the prediction errors exceed a few hours and consequently, transit events can no longer be reliably observed during a single night. For the SRc01 fields, photometric follow-up was performed with the 0.8 m telescope in Observatorio del Teide (Spain) from the Instituto de Astrofsica de Canarias (hereafter IAC80), with the 1.2 m Euler telescope in La Silla Observatory (Chile) from the Geneva Observatory and with the 1m telescope at the Wise Observatory (Israel) from Tel-Aviv University (see Table 1).

5.1.2. Radial velocity follow-up

Radial velocity (RV) follow-up is needed to identify the nature of the transiting object and establish the mass of the planet and the eccentricity of its orbit. This can be done by measuring the RV variations of a star caused by the presence of a companion. Such an RV variation is directly linked to the mass ratio of the main star to its companion object. Radial velocities are obtained by a weighted cross-correlation function (hereafter CCF) between a numerical spectral mask (see Baranne et al. 1996; Pepe et al. 2002) and a stellar spectrum taken with the SOPHIE spectrograph, mounted on the 1.93 m telescope in Observatoire de Haute-Provence (France), with the HARPS spectrograph mounted on the ESO-3.6 m telescope in the ESO La Silla Observatory (Chile) and with the FLAMES/UVES spectrograph, mounted on the VLT UT2 telescope in the ESO Paranal Observatory (Chile) (see Table 1). Both SOPHIE and HARPS are fiber-fed echelle spectrographs with a resolution of between about 39 000 (SOPHIE, high efficiency mode) and 110 000 (HARPS, high accuracy mode) at 550 nm. Observations of SOPHIE and HARPS were obtained using the observing mode Obj_AB without acquisition of a simultaneous thorium lamp spectrum to monitor the Moon background light in the second fibre. The intrinsic stability of these spectrographs does not require the use of lamp calibration spectra, the instrumental drift during one exposure being in our case always smaller than the stellar RV photon noise uncertainties. The FLAMES spectrograph contains a multi fiber-link, which makes it possible to feed up to seven targets and a ThAr calibration lamp into the UVES echelle spectrograph with a resolution of about 47 000 at 550 nm (Loeillet et al. 2008; Bouchy et al. 2005).

In the magnitude range of the CoRoT targets, RV uncertainties are mostly dominated by photon noise limitation (Santerne et al. 2011). Thus, the RV follow-up with SOPHIE and HARPS was mainly concentrated on candidates with priority 1 and 2 and a V-magnitude brighter than 16. Taking advantage of the large aperture of ESO-VLT/FLAMES facilities, we followed up some priority 3 and 4 candidates or candidates fainter than the above magnitude limit in the FLAMES fields.

5.2. Results of the follow-up observations

Ground-based follow-up observations were performed for 26 of the 51 transit candidates in the SRc01 field (see Table 10), including all three priority 1 candidates and the eleven candidates in priority 2 brighter than $m_V \sim 16$. On the basis of these observations, it was possible to conclude a non-planetary nature for seven of the candidates (four spectroscopic binaries, two contaminating or background eclipsing binaries, and one blended binary system). Furthermore, nine targets are found to be hot or rapidly rotating stars for which we not can obtain precise enough RV measurements to determine their nature. For five cases, it was possible to estimate an upper limit to the mass of a potential companion. The remaining candidates are still unresolved mainly owing to the photon noise limitation or ephemeris uncertainties mentioned above. For instance among the 18 high priority cases (class 1 and 2), eight remain unresolved and are good planetary candidates pending future detailed investigation.

We now discuss the follow-up results below. For each candidate we provide the CoRoT win-ID, acquisition mode (monochromatic (MON) or chromatic (CHR) band), and CoRoT-ID.

5.2.1. Priority 1 candidates

SRc01 E1 0936 – MON – 0211645912

For this target, the CoRoT data show a variable lightcurve with an amplitude of 0.7% and a period of 3.93 days; superimposed on this, there are transit-like events with a period of 5.1 days (see Fig. 2). On-off photometry with Euler in R-filter indicates a blend of three stars. From CoRoT photometry, one cannot determine which of the three stars is responsible for either the transit-like events or the variability; but given the amplitudes of the effects and the relative fluxes of the stars, one can calculate the

Table 2. Radial-velocity measurements of E1 0936 composant B. EGGS is the high efficiency mode of HARPS.

BJD-2 400 000	RV [km s^{-1}]	σ [km s^{-1}]	Instrumental mode
	HARPS		
54 701.67678	17.0424	0.0834	EGGS
54 702.55488	17.2316	0.0414	EGGS
54 705.62280	17.1783	0.0673	EGGS
54 705.65396	17.2002	0.0367	EGGS

expected on-target amplitudes that, blended, will be compatible with CoRoT measurements. If one assigns A, B, and C to these stars, the flux ratios are $A/B \sim 1.5$ and $B/C \sim 19$. Thus, if star A were to be responsible for the transits, one would observe transits 0.43% deep; for star B, the depth would be 0.64% and for star C the transit would be 12% deep. For the variability, if star A were responsible for the variability, the amplitude would be 1.2%, whereas it would be 1.8% in the case of star B, and 34% in the case of star C. Aperture photometry shows no evidence of any nearby eclipsing binary. The resulting light curves of the on-off photometric measurements indicate that A and B are constant to within the 1% level, whereas C is variable at the 20% level. There is maybe a hint of an eclipse event on A, but the photometry is too imprecise for us to draw any firm conclusions. Even the variability of C could be an artifact. Both stars A and B were followed up with HARPS: star A showed no peak in the CCF, which would be indicative of either a hot or fast-rotator star; star B does not show any significant RV variation in phase with the CoRoT ephemeris up to 80 m/s (see Table 2). The nature of this candidate remains unresolved. If the transit is on star A, the case cannot be solved because of the nature of the host star. If the transit occurs in star B, the upper limit to the mass of the hypothetical companion would be 0.6 $M_{\rm Jup}$.

SRc01 E1 1773 – MON – 0211660040

CoRoT data reveal the presence of a 0.96% deep transit with a period of 16.2 days. Additional stellar activity is also seen with a characteristic period of 1.35 days. Subsequent ground-based follow-up observations were performed with SOPHIE and HARPS from June to September 2008 (see Table 3 and Fig. 4). For the observational data at hand, the cross-correlation function (CCF) has a single peak with a vsini of about 6.6 ± 1.0 km s^{-1}. The mean errors in the radial velocity measurement are about 45 m/s. An analysis of the RV data indicates a drift of about 3.8 m/s per day over 60 days with a possible asymmetry in the stellar line profile. This implies that there is a binary system blended in the HARPS point spread function (PSF). On the other hand, we could not detect any significant RV variations in the residual in-phase with the transit ephemeris or activity. The DSS2 skychart from Aladin shows that at least four stars contribute to the flux measured in the CoRoT mask. Photometric follow-up of the transit event with the IAC80 was missed by a few hours owing to the large ephemeris uncertainties. The target was also observed with the Wise 1m telescope, with no filter, at ~43 degrees from the full Moon. A partial lunar eclipse occurred during this observation. The transit and/or the stellar activity could be due to one of the contaminants. Thus, the exact nature of the candidate remains unresolved, pending future photometric observations.

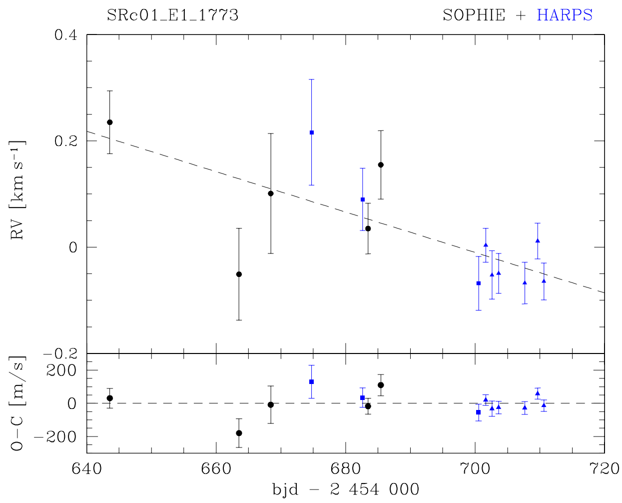

Fig. 4. Radial velocity measurements of E1 1773 with SOPHIE (black points) and HARPS – HAM (blue square) and HARPS – EGGS (blue triangle).

Table 3. Radial-velocity measurements of E1 1773.

BJD-2 400 000	RV [km s^{-1}]	σ [km s^{-1}]	BIS [km s^{-1}]	Instrumental mode
		SOPHIE		
54 643.56975	46.422	0.0590	0.0123	HE
54 663.52737	46.136	0.0864	0.0212	HE
54 668.42729	46.288	0.1129	0.0066	HE
54 683.45760	46.222	0.0476	0.0180	HE
54 685.43381	46.342	0.0643	–0.0098	HE
		HARPS		
54 674.73936	46.224	0.0995	–0.0493	HAM
54 682.61512	46.098	0.0586	0.0761	HAM
54 700.53167	45.940	0.0507	0.2478	HAM
54 701.63179	46.015	0.0317	0.0030	EGGS
54 702.60073	45.959	0.0455	0.0751	EGGS
54 703.63499	45.962	0.0376	0.0246	EGGS
54 707.66147	45.944	0.0393	0.0808	EGGS
54 709.65100	46.023	0.0336	0.1083	EGGS
54 710.61748	45.947	0.0346	0.0925	EGGS

Notes. HE is the high efficiency mode of SOPHIE. HAM is the high accuracy mode of HARPS. BIS is the slope of the bisector span. Uncertainties in the bisector is estimated to be twice the uncertainties of radial velocity.

SRc01 E1 3315 – MON – 0211662780

The candidate E1 3315 displays a 1.0% deep transit with a period of 4.551 days. FLAMES observations were acquired on 9 and 10 June 2008 and the star then displayed a variation of 15 km s^{-1} between phase 0.02 and 0.21. This result is indicative of a spectroscopic binary (SB1) with a secondary mass of about 130 $M_{\rm Jup}$, assuming a solar-mass primary star.

5.2.2. Priority 2 candidates

SRc01 E1 2630 – MON – 0211630451

CoRoT detects 0.46% deep transits with a period of 1.5943 days for this candidate. The star was observed three times with HARPS from 20 to 23 August 2009 (see Table 4). With radial velocity uncertainties ranging from 40 to 80 m/s, we could not detect any significant RV variation at the CoRoT ephemeris. If on target, this result places an upper limit on the mass of the

Table 4. Radial-velocity measurements of E1 2630.

BJD-2 400 000	RV [km s^{-1}]	σ [km s^{-1}]	Instrumental mode
HARPS			
55 063.61054	–23.1961	0.0827	HAM
55 064.64912	–23.0967	0.0401	HAM
55 066.59265	–23.1767	0.0526	HAM

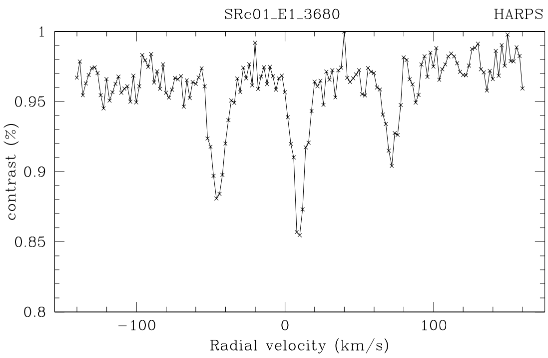

Fig. 5. Result of the CCF between the HARPS spectrum of E1 3860 and a G2 mask. The three peaks indicate the presence of three stars in this system.

companion of 0.5 $M_{\rm Jup}$, assuming a solar mass star. Thus, the nature of this candidate remains unresolved.

SRc01 E1 3860 – MON – 0211635507

For the candidate E1 3860 with a 2.5% deep and a period of 21.238 days, one HARPS spectrum was acquired on 25 July 2008. The cross-correlation function (see Fig. 5) indicates a spectroscopic binary of type 3 (SB3), with components separated by 50 and 60 km s^{-1}. Thus, one exposure was sufficient to discard this candidate as an eclipsing binary diluted by a third star. That the eclipses measured by CoRoT, which are already 2.5% deep, are diluted by the light of two stars makes the planet hypothesis unlikely.

SRc01 E2 1822 – MON – 0211642286

This priority 2 candidate shows shallow (0.25%) eclipses with a period of 0.94 days. IAC80 photometric follow-up data found no evidence of any nearby eclipsing binary, but the ephemeris at the time of the observations had large errors (estimated 2 h). With a m_R of 15.8, this candidate is too faint for precise enough RV measurements. The nature of the candidate remains unclear.

SRc01 E1 2700 – MON – 0211650167

Ground-based follow-up observations for E1 2700 were performed with SOPHIE on 27 June 2008. No peak in the CCF was detected and the spectrum contains only Balmer lines. The target is also a hot star or a very fast rotator making accurate radial velocity measurements difficult. The nature of the 0.37% deep transit event with a 2.857 days period found by CoRoT remains unresolved.

SRc01 E1 3691 – MON – 0211651069

The candidate E1 3691, with a 0.35% transit and a 2.763 days period was observed with HARPS on 23 August 2009. No peak in the CCF was detected. The target is also a hot star or a very fast rotator. The cause of the transit could not be determined by RV measurements.

SRc01 E1 2322 – MON – 0211657825

The candidate E1 2322 has a 0.35% deep and 2.246 days period and was observed with HARPS on 21 and 24 June 2009. A first analysis of the CCF shows a single peak caused by Moon background light contamination. After correcting this contamination, there is no longer a peak in the CCF, which indicates that the target is also a hot star or a very fast rotator, thereby making precise RV measurements difficult. Unfortunately, a later reanalysis of the photometric CoRoT lightcurve revealed that the light from the bright eclipsing binary SRc01 E1 0198 contaminated the nearby masks of the candidates E1 2322 (at 27″) and E1 4746 (at 16″), because both share the ephemeris of the eclipsing binary. Therefore, these candidates were resolved with the help of CoRoT on-off photometry. This is one of the consequences of the severe crowding of this particular area in the SRc01 field and was not realized at an earlier stage of the mission because of an underestimate of the importance of the contamination. The eclipsing binary contributes only 0.7% of the flux within the mask of E1 4746 and only 0.3% in the case of E1 2322, but this small contribution is still enough to produce a false detection, because of the high precision of the measurements.

SRc01 E2 2046 – MON – 0211660744

This transit candidate has a 0.28% deep and a 0.821 days period. Photometric follow-up observations were done with the IAC80 telescope in April 2009. Two close neighbors (separation ≤ 3″) could be excluded as possible contaminants and no deep eclipses were found in any nearby stars. Given the faintness of the target (m_R = 15.6) and the extremely shallow transit found in the CoRoT data, it was impossible to resolve this case with the performed observations.

SRc01 E2 0338 – CHR – 0211662131

In the CoRoT data of E2 0338, a transit event with 0.26% depth and a period of 6.098 days was found. The candidate was observed with FLAMES on 10 June 2008. Two peaks are present in the CCF that indicate a clear SB2. One exposure was thus sufficient to identify this candidate as an eclipsing binary. We did not attempt to constrain the secondary mass with a second measurement, nor to check whether the velocity variation was in-phase with the CoRoT ephemeris. The lightcurve shows an additional transit-like event at the epoch 2 454 221.2 with a depth of 0.7% in the blue channel, which was invisible in the red or green channels, which indicates that this event occurs in a background object, probably a long-period eclipsing binary.

SRc01 E1 3835 – MON – 0211666030

From CoRoT, the candidate E1 3835 has a 0.51% deep transit event with a period of 2.261 days. The candidate was observed with HARPS on 22 June 2008 showing a vsini of about 2.5 ± 1.0 km s^{-1} (see Table 5). Later photometric on-off observations with the IAC80 revealed that a 1.1 mag fainter star located 10″ NW of the CoRoT target had a 5% deep eclipse at the CoRoT ephemerides. These observations are consistent with the

Table 5. Radial-velocity measurements of E1 3835.

BJD-2 400 000	RV [km s^{-1}]	σ [km s^{-1}]	Instrumental mode
	HARPS		
54 640.81451	6.0980	0.1390	HAM

Table 6. Radial-velocity measurements of E1 2059.

BJD-2 400 000	RV [km s^{-1}]	σ [km s^{-1}]	Instrumental mode
	SOPHIE		
54 680.45699	–18.7321	0.0889	HE
	HARPS		
54 702.64461	–19.3387	0.0594	EGGS
54 709.58332	–19.2998	0.0484	EGGS

Table 7. Radial-velocity measurements of E1 0780.

BJD-2 400 000	RV [km s^{-1}]	σ [km s^{-1}]	Instrumental mode
	SOPHIE		
54 644.55773	–17.2907	0.1193	HE
54 665.49116	–17.3629	0.1107	HE
54 682.42782	–17.2822	0.0297	HE
	HARPS		
54 700.61608	–17.2990	0.0220	HAM
54 705.59475	–17.2373	0.0229	HAM
54 709.54263	–17.2170	0.0239	HAM

observed transit depth found by CoRoT (Deeg et al. 2009), so this candidate was discarded as a background eclipsing binary.

SRc01 E1 2059 – MON – 0211670576

From the CoRoT observations, a 0.20% deep transit with a period of 2.732 days was found for E1 2059. The candidate was observed with both SOPHIE and HARPS in July and August 2008 (see Table 6). With radial velocity uncertainties ranging from 40 to 90 m/s, we could not detect any significant RV variation in the CoRoT ephemeris implying that the upper limit to the mass of an hypothetical companion is 0.4 $M_{\rm Jup}$. From HARPS CCF, the vsini estimate is about 2.2 ± 1.0 km s^{-1}. Thus, the nature of this target remains unclear.

SRc01 E1 4522 – MON – 0211676514

This candidate was observed with HARPS on 26 and 28 June 2008. We found different amplitudes in the radial velocity signal depending on the cross-correlation mask (according to Bouchy et al. 2009). The largest value was determined for the F0 mask, implying an early-type primary star in a blended binary system. The velocity variation in the blended binary is in-phase with the CoRoT ephemeris. Thus, the diluted eclipses of this double star are the origin of the 0.38% deep photometric signal with a period of 1.391 days found by CoRoT.

5.2.3. Priority 3 candidates

SRc01 E1 0346 – MON – 0211620782

CoRoT observations of the candidate E1 0346 found a 0.45% deep event with a period of 14.499 days. Subsequent follow-up observations were performed with HARPS on 21 August 2008 without detecting any peak in the CCF. The target is either a hot star or a very fast rotator and precise radial velocity measurements are impossible. The cause of this event remains unclear and no planetary mass could be characterized for this target.

SRc01 E1 0507 – CHR – 0211626061

In the same way as for the previous candidate, HARPS observations took place on 21 August 2008 for this 0.25% deep candidate with a period of 6.409 days. No peak in the CCF was detected for the target and the case remains unresolved. The star is also either a hot star or a very fast rotator for which we not can measure a planetary mass companion.

SRc01 E1 3584 – MON – 0211643311

Follow-up observations of the candidate E1 3584, with a depth of 0.64% and a period of 4.239 days were performed with FLAMES on 10 June 2008. No peak in the CCF was detected in the data. The target is either a hot star or a very fast rotator, hence precise RV measurements are not possible. The true nature of the candidate remains unclear.

SRc01 E1 3468 – MON – 0211647986

The candidate E1 3468 was also observed with FLAMES on 10 June 2008 but no peak was detected in the CCF. As in the previous case, this is either a hot star or a very fast rotator thereby limiting the precision of the radial velocity measurements. The cause of the 1.2% deep event with a period of 2.037 days found in the CoRoT data could not be resolved.

SRc01 E2 1288 – MON – 0211650063

CoRoT observed a single transit event with a depth of 1.7% for this candidate with a minimal period of about 18 days. Follow-up observations were performed with FLAMES on 10 and 12 June 2008. The data obtained shows a variation of 5 km s^{-1} indicating a SB1 system with a minimum mass for the invisible companion of 200 $M_{\rm Jup}$.

SRc01 E2 0713 – MON – 0211657608

This candidate, with a depth of 0.11% and a period of 2.003 days was also observed with FLAMES on 10 and 12 June 2008 (phases close to 0.94 and 0.86, respectively) and shows a variation of 2.2 km s^{-1} but not in phase with the CoRoT ephemeris. These two measurements are insufficient to conclude anything about this target's nature. Thus, the nature of this candidate remains unclear pending new RV measurements.

SRc01 E2 1283 – MON – 0211663583

This candidate with a depth of 0.3% and a period of 2.458 days was also observed with FLAMES on 10 and 12 June 2008 (phases close to 0.35 and 0.1, respectively) and shows a variation of 1.4 km s^{-1} but not in phase with the CoRoT ephemeris. From the two measurements, it was impossible to determine on the cause of the transit event. Thus, the candidate remains unresolved pending new RV measurements.

SRc01 E1 2420 – MON – 0211670372

FLAMES observations for E1 2420 were acquired on 9 June and no peak in the CCF was detected. In addition, the target is either a hot or a very fast rotating star making precise radial velocity

Table 8. Radial-velocity measurement of E1 4599.

BJD-2400000	RV [km s^{-1}]	σ [km s^{-1}]	Instrumental mode
HARPS			
55 063.65399	28.2095	0.7238	HAM

Table 9. Radial-velocity measurements of E1 2291.

BJD-2 400 000	RV [km s^{-1}]	σ [km s^{-1}]	Instrumental mode
HARPS			
54 675.73024	–43.0609	0.0385	HAM
54 679.66430	–42.9828	0.0561	HAM
54 681.65859	–42.9630	0.0431	HAM

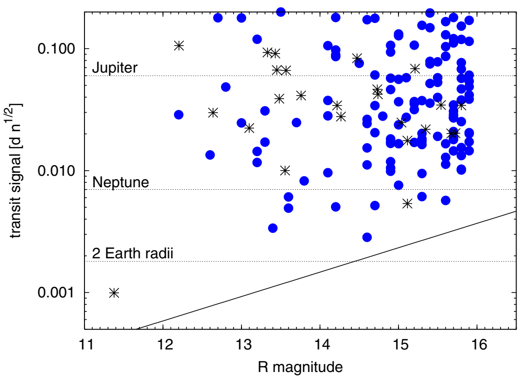

Fig. 6. Transit signal vs. R magnitude for the objects described in this paper. The asterisks represent the position of the planets as well as two brown-dwarfs discovered by CoRoT (CoRoT-7b is in the bottom left corner). For comparison the horizontal dashed lines represent (from top to bottom) the expected signal produced by a Jupiter-size planet, a Neptune-size planet, and a 2 Earth-radii planet, respectively orbiting a solar-like star at a short period.

measurements challenging. Thus, the cause of the detected 0.6% event with a period of 2.161 days remains unclear.

5.2.4. Priority 4 candidates

SRc01 E1 0780 – CHR – 0211628697

The target E1 0780 was observed with both SOPHIE and HARPS during summer 2008 (see Table 7) to investigate the nature of this relatively bright candidate (m_R = 14.1), which shows a 0.14% deep transit with a period of 2.434 days in the CoRoT data. From the HARPS data, we found a vsini of about 5.9 ± 1.0 km s^{-1} and RV uncertainties of about 20 m/s for three observations. No significant variation was found in phase with the CoRoT ephemeris, corresponding to an upper limit in mass of 0.3 $M_{\rm Jup}$ for a companion. The cause of the events hence remains unresolved.

SRc01 E1 1078 – MON – 0211647475

CoRoT detected a single 0.65% transit with a total duration of 25 h. This mono-transit candidate was observed in the field of FLAMES/GIRAFFE observations for stellar characterization of the CoRoT exoplanet fields (Gazzano et al. 2010). The acquired spectrum is compatible with a hot star but no precise radial velocities could be obtained. The cause of this single transit cannot be established with the instrumentation used.

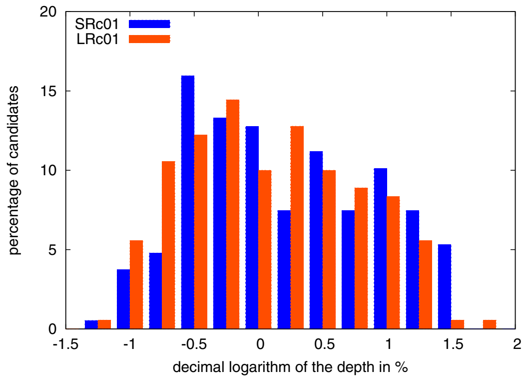

Fig. 7. Histogram with a comparison of the depths of the detections found in the SRc01 and LRc01 runs.

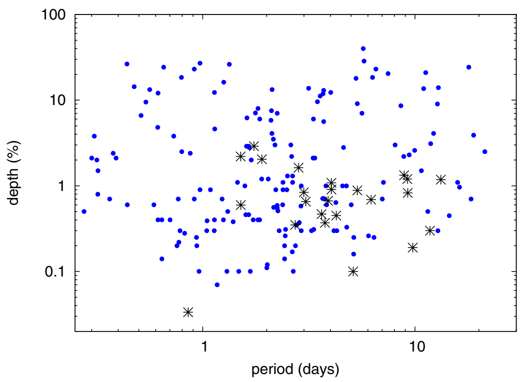

Fig. 8. Periods vs. depths for the objects found in the SRc01 field. The asterisks represent the position of the planets and two brown-dwarfs discovered by CoRoT, except CoRoT-9b.

SRc01 E1 4599 – MON – 0211663968

CoRoT detected a 0.26% transit event with a period of 2.450 days for E1 4599. A subsequent ground based follow-up observation was performed with HARPS on 19 August 2009 (see Table 8). The CCF shows a noisy peak with a vsini of about 6.5 ± 1.0 km s^{-1} and a contrast of 4.8%, which gave a radial velocity uncertainty of about 0.7 km s^{-1}. The faint CCF area suggests that the observed spectrum is diluted by a brighter hot or fast-rotating star. A second observation is planned with lower priority owing to the low precision measurements available with HARPS. At present, the cause of the detected events remains unclear.

SRc01 E1 2291 – MON – 0211664319

The candidate E1 2291 with a 0.10% deep event and a period of 2.667 days was observed with HARPS three times in July and August 2008 (see Table 9). With radial velocity uncertainties ranging from 40 to 60 m/s, no significant RV variation at the CoRoT ephemeris could be detected, which is compatible with a upper limit in mass of about 0.2 $M_{\rm Jup}$ for a companion. The cause of the event observed by CoRoT is unclear.

6. Discussion

Among the 6974 SRc01 targets observed by CoRoT, we have found 51 transit candidates and 139 eclipsing binaries. As summarized in Table 10, ground-based follow-up observations were initiated for 26 of the candidates, including a large part of the

Table 10. Planetary transit candidates in the CoRoT SRc01 field.

Pr	CoRoTid	Winid	Right ascension (J2000.0)	Declination (J2000.0)	B	R	Period(d)	Epoch (HJD-2 454 000)	Depth (%)	Length (h)	Follow-up result
1	0211645912	E1_0936	19 03 16.94	3 04 48.5	15.2	14.9	5.1469 ± 0.0015	206.8506 ± 0.0043	0.25	3.2	hot star/no variation
1	0211660040	E1_1773	19 04 02.67	2 03 18.0	15.5	14.7	16.2018 ± 0.0044	209.2497 ± 0.0029	0.96	5.7	not resolved
1	0211662780	E1_3315	19 04 10.77	2 09 09.0	16.3	15.9	4.5513 ± 0.0010	208.8077 ± 0.0020	1.0	2.1	SB1
2	0211627014	E1_3942	19 01 57.59	3 02 06.0	17.8	15.7	1.85067 ± 0.00079	205.3927 ± 0.0053	0.40	3.9	
2	0211630451	E1_2630	19 02 14.47	2 05 33.2	16.4	15.3	1.59431 ± 0.00031	205.9354 ± 0.0027	0.46	1.8	not resolved
2	0211631779	E2_1625	19 02 21.02	3 34 47.8	18.3	15.8	single transit	213.8410 ± 0.0050	1.8	10.3	
2	0211635507	E1_3860	19 02 37.44	1 54 08.4	18.2	15.9	21.328 ± 0.020	205.5880 ± 0.0050	2.5	3.0	SB3
2	0211641087	E1_3314	19 03 00.06	3 08 23.4	16.3	15.4	2 x single transit	211.3940 ± 0.0050	1.4	4.5	
2	0211642286	E2_1822	19 03 04.28	3 14 31.8	18.8	15.8	0.93512 ± 0.00076	209.6168 ± 0.0072	0.25	2.4	not resolved
2	0211649312	E1_3946	19 03 28.48	2 37 25.7	16.8	15.6	single transit	212.3920 ± 0.0050	1.2	10.7	
2	0211650167	E1_2700	19 03 31.40	2 55 12.9	16.0	14.9	2.85665 ± 0.00034	206.2185 ± 0.0050	0.37	2.9	hot star
2	0211651069	E1_3691	19 03 34.52	2 22 06.6	18.5	15.6	2.7636 ± 0.0014	205.1906 ± 0.0072	0.35	3.2	hot star
2	0211657825	E1_2322	19 03 56.05	2 42 50.5	15.7	15.3	2.2467 ± 0.0065	205.8778 ± 0.0679	0.55	6.6	contaminating ecl. binary
2	0211660744	E2_2046	19 04 04.66	3 37 30.6	18.7	15.6	0.82059 ± 0.00030	210.6863 ± 0.0039	0.28	3.0	on target
2	0211662131	E2_0338	19 04 08.84	3 18 00.5	15.1	12.6	6.0476 ± 0.0063	211.4302 ± 0.0085	0.26	3.8	SB2
2	0211666030	E1_3835	19 04 19.67	2 59 26.1	17.5	15.7	2.26051 ± 0.00054	204.8119 ± 0.0036	0.51	4.0	background ecl. binary
2	0211670576	E1_2059	19 04 31.33	2 27 00.4	15.9	14.6	2.73208 ± 0.00046	205.8121 ± 0.0067	0.20	4.4	not resolved
2	0211676514	E1_4522	19 04 46.04	2 15 27.9	18.3	15.5	1.39111 ± 0.00038	205.3112 ± 0.0080	0.38	3.6	blended binary system
3	0211620782	E1_0346	19 01 24.10	2 41 39.0	13.6	12.2	14.4993 ± 0.0067	212.3962 ± 0.0046	0.45	5.8	hot star
3	0211626061	E1_0507	19 01 52.52	2 06 09.7	14.3	13.2	6.4093 ± 0.0026	209.2348 ± 0.0051	0.25	3.1	hot star
3	0211634383	E2_1066	19 02 32.79	3 16 47.1	18.9	15.7	single transit	215.6940 ± 0.0050	4.0	66	
3	0211635059	E1_4500	19 02 35.70	3 07 12.0	17.4	15.8	2.50906 ± 0.00055	207.2504 ± 0.0024	1.3	3.9	
3	0211643311	E1_3584	19 03 07.74	2 53 16.0	16.1	15.8	4.2388 ± 0.0020	208.5266 ± 0.0050	0.64	5.0	hot star
3	0211647986	E1_3468	19 03 23.99	2 47 19.6	16.2	15.0	2.03712 ± 0.00027	206.5495 ± 0.0014	1.2	3.1	hot star
3	0211650063	E2_1288	19 03 31.07	3 29 32.3	16.6	14.2	single transit	227.8710 ± 0.0050	1.7	16	SB1
3	0211652780	E2_1282	19 03 40.11	3 25 44.6	17.8	14.9	5.1385 ± 0.0065	212.001 ± 0.017	0.16	5.4	
3	0211654624	E1_0257	19 03 45.97	2 50 30.2	17.1	14.7	1.67754 ± 0.00056	204.9441 ± 0.0041	0.10	3.8	
3	0211657608	E2_0713	19 03 55.40	3 31 42.0	18.5	15.6	2.0032 ± 0.0011	211.3196 ± 0.0055	0.11	3.8	not resolved
3	0211658476	E2_2114	19 03 58.01	3 40 48.6	18.1	15.7	1.04705 ± 0.00033	210.9780 ± 0.0030	0.39	3.3	
3	0211661899	E1_3525	19 04 08.17	3 08 11.6	16.6	15.1	4.774 ± 0.003	205.449 ± 0.009	0.33	9.8	
3	0211662267	E1_1393	19 04 09.24	2 42 02.9	15.5	15.3	2.0174 ± 0.0011	206.2918 ± 0.0098	0.12	3.7	

Table 10. continued.

Pr	CoRoTid	Winid	Right ascension (J2000.0)	Declination (J2000.0)	B	R	Period(d)	Epoch (HJD-2 454 000)	Depth (%)	Length (h)	Follow-up result
3	0211662665	E1_1383	19 04 10.42	2 24 45.5	15.5	14.8	2.89727 ± 0.00047	206.0033 ± 0.0020	0.58	3.3	
3	0211663583	E2_1283	19 04 13.07	3 23 09.9	17.3	15.0	2.45844 ± 0.00078	211.7682 ± 0.0028	0.31	4.1	not resolved
3	0211666578	E1_2550	19 04 21.11	2 37 40.5	15.8	15.5	single transit	208.412 ± 0.011	0.93	10.	
3	0211667173	E1_4570	19 04 22.66	3 02 05.7	18.1	15.9	3.6729 ± 0.0014	205.1731 ± 0.0049	0.71	4.9	
3	0211668033	E1_3304	19 04 24.90	2 54 24.0	18.0	15.8	0.77196 ± 0.00083	205.2587 ± 0.0016	0.22	3.0	
3	0211668801	E1_2625	19 04 26.99	2 28 40.0	16.0	15.0	1.64622 ± 0.00025	205.9347 ± 0.0023	0.46	3.8	
3	0211670372	E1_2420	19 04 30.89	2 00 42.5	16.0	14.9	2.16053 ± 0.00025	204.7040 ± 0.0016	0.56	1.5	hot star
3	0211674653	E1_3350	19 04 41.40	2 16 31.1	16.4	15.7	3.3349 ± 0.0014	204.9884 ± 0.0052	0.31	4.8	
4	0211606052	E2_1663	18 59 38.88	3 15 03.4	17.5	15.9	3.250 ± 0.0038	211.647 ± 0.0010	0.30	4.7	
4	0211616889	E1_1057	19 01 00.06	2 07 05.4	16.0	14.2	single transit	216.0950 ± 0.0050	0.63	34.	
4	0211621528	E1_0520	19 01 28.40	3 05 01.2	15.8	13.3	single transit	220.9630 ± 0.050	0.40	8.5	
4	0211626526	E1_4557	19 01 55.06	2 06 08.7	17.4	15.9	0.440893 ± 0.000038	204.6891 ± 0.0012	0.60	1.6	
4	0211628697	E1_0780	19 02 05.91	2 13 05.8	16.7	14.1	2.433707 ± 0.004924	211.160511 ± 0.024865	0.14	6.7	not resolved
4	0211647475	E1_1078	19 03 22.25	2 52 23.8	15.4	14.2	single transit	224.3370 ± 0.050	0.65	25.	hot star
4	0211658113	E1_4746	19 03 56.95	2 43 09.2	16.9	15.2	2.2457 ± 0.0010	205.8540 ± 0.0070	0.59	4.1	
4	0211663835	E1_1099	19 04 13.70	2 40 32.5	17.3	13.4	1.1697 ± 0.0014	205.329 ± 0.013	0.07	3.3	
4	0211663968	E1_4599	19 04 14.12	2 42 33.5	18.0	15.9	2.449926 ± 0.009576	210.673138 ± 0.048357	0.26	8.8	not resolved / blend?
4	0211664319	E1_2291	19 04 15.03	2 47 15.2	15.8	15.0	2.666830 ± 0.005581	210.790627 ± 0.024960	0.10	8.2	not resolved
4	0211665710	E1_2669	19 04 18.82	2 46 11.5	15.9	14.9	2.64986 ± 0.00053	205.5553 ± 0.0027	1.3	9.5	
4	0211666773	E1_2615	19 04 21.61	2 46 46.8	16.0	15.3	2.6441 ± 0.0015	205.5925 ± 0.0048	0.17	4.4	

Table 11. Eclipsing binaries found in SRc01.

CoRoTid	Winid	Right ascension (J2000.0)	Declination (J2000.0)	*B*	*R*	Period(d)	Epoch (HJD-2 454 000)	Length (h)	Depth (%)
0211609276	E2_1262	19 00 04.99	3 53 46.7	17.8	15.0	2.389647 ± 0.000412	212.030461 ± 0.001407	2.36	0.9
0211656097	E1_3613	19 03 50.70	2 51 48.2	17.3	15.2	4.276980 ± 0.001947	207.501612 ± 0.005206	4.60	0.3
0211642815	E2_2022	19 03 06.13	3 45 29.4	18.6	15.0	10.716990 ± 0.011521	217.225965 ± 0.007733	11.0	1.5
0211662206	E2_2013	19 04 09.06	3 18 54.7	19.8	15.9	4.149360 ± 0.001341	212.250814 ± 0.003414	3.36	0.3
0211636271	E1_4162	19 02 40.68	2 20 08.7	17.2	15.8	1.695746 ± 0.000157	205.555556 ± 0.001287	2.09	2.0
0211630144	E1_4046	19 02 12.87	2 58 04.1	19.4	15.6	2.601250 ± 0.000183	206.151889 ± 0.000993	2.67	3.0
0211630988	E1_4119	19 02 16.97	3 02 18.8	17.6	15.4	2.209523 ± 0.000527	206.283882 ± 0.003267	4.71	0.9
0211661480	E1_0303	19 04 06.89	2 17 59.1	13.2	12.8	7.101574 ± 0.000940	209.508062 ± 0.001121	2.77	1.1
0211663951	E1_2856	19 04 14.07	2 44 06.2	15.9	15.4	11.504968 ± 0.010803	214.630800 ± 0.006728	7.25	0.5
0211614750	E1_0554	19 00 45.47	2 12 56.6	19.1	15.6	2.430667 ± 0.001100	206.577051 ± 0.006840	4.51	0.2
0211647819	E2_2240	19 03 23.43	3 27 32.2	18.2	15.9	3.763383 ± 0.001916	212.595419 ± 0.003931	8.5	0.7
0211660858	E2_0369	19 04 04.98	3 24 46.4	14.3	12.7	8.841224 ± 0.008798	218.672545 ± 0.008260	9.43	2.2
0211665098	E2_1124	19 04 17.18	3 31 14.2	17.6	14.9	1.819895 ± 0.000399	211.450387 ± 0.002125	2.65	0.4
0211670565	E1_3701	19 04 31.30	2 47 18.0	16.2	15.5	2.492569 ± 0.000251	205.897652 ± 0.001149	2.79	0.9
0211626880	E1_2395	19 01 56.80	2 59 47.7	19.2	15.8	2.293119 ± 0.000585	206.374453 ± 0.002960	3.78	0.3
0211630490	E2_1093	19 02 14.69	3 28 22.3	16.9	15.2	1.604609 ± 0.000121	210.990263 ± 0.000712	1.93	2.9
0211644671	E1_1696	19 03 12.62	2 46 11.0	15.8	14.6	1.250148 ± 0.000180	205.723314 ± 0.001845	5.25	0.4
0211649857	E1_1194	19 03 30.37	2 20 21.5	14.8	14.9	1.458794 ± 0.000075	205.309031 ± 0.000642	2.52	1.1
0211650675	E1_0640	19 03 33.11	2 13 33.2	15.0	14.1	0.971758 ± 0.000084	205.117305 ± 0.001212	2.49	0.9
0211656648	E2_2083	19 03 52.45	4 07 58.9	18.7	15.7	3.375015 ± 0.000430	212.406617 ± 0.001199	4.0	2.1
0211612920	E1_0678	19 00 32.57	1 49 01.7	17.0	15.4	3.716464 ± 0.000222	208.568981 ± 0.000853	5.5	5.6
0211622702	E1_3741	19 01 34.97	1 50 38.6	16.9	15.5	12.246834 ± 0.001993	211.958452 ± 0.001550	4.3	4.1
0211642487	E1_2591	19 03 04.94	3 04 59.6	16.7	15.2	7.023783 ± 0.001577	208.837599 ± 0.002374	3.94	0.7
0211649707	E1_0564	19 03 29.91	2 33 39.4	14.8	13.2	2.119429 ± 0.000948	206.814155 ± 0.005714	3.02	0.5
0211652774	E1_2964	19 03 40.09	2 02 40.7	16.2	15.3	2.150551 ± 0.000139	205.864028 ± 0.001028	2.8	3.5
0211657002	E1_2435	19 03 53.53	2 11 33.2	16.1	15.4	0.613927 ± 0.000027	204.903295 ± 0.000657	3.5	4.8
0211659543	E1_3427	19 04 01.16	2 44 37.7	18.5	15.5	1.580258 ± 0.000202	206.054335 ± 0.001853	4.73	1.0
0211660294	E2_1917	19 04 03.38	3 31 23.7	17.4	15.2	1.311428 ± 0.000443	211.070435 ± 0.003551	7.09	0.5
0211663923	E1_1760	19 04 13.99	2 46 39.4	15.2	13.6	12.737937 ± 0.002185	215.431808 ± 0.000941	5.83	9.0
						5.298273 ± 0.005652	205.56170 ± 0.001413	8.2	0.3
0211676168	E1_1702	19 04 45.15	2 08 48.0	15.9	15.7	3.829713 ± 0.000461	207.022105 ± 0.001596	2.95	0.6
0211604558	E1_0546	18 59 26.31	2 36 31.4	15.7	13.6	1.334376 ± 0.000052	205.595663 ± 0.000540	8.24	26.1
0211607375	E1_4360	18 59 49.70	1 49 22.8	16.7	15.4	10.999711 ± 0.007577	213.436303 ± 0.006498	5.11	13.6
0211607781	E1_3410	18 59 52.91	2 45 13.4	17.9	15.7	0.320139 ± 0.000017	204.877656 ± 0.000780	2.65	0.8
0211608608	E1_2282	18 59 59.64	2 38 30.9	17.3	15.3	11.238132 ± 0.002323	211.98510 ± 0.00156	8.7	21.
0211610659	E1_1766	19 00 15.64	3 03 23.5	16.8	14.7	0.971547 ± 0.000067	205.332472 ± 0.000934	8.6	27.
0211611561	E2_0822	19 00 22.50	3 16 46.4	18.0	15.0	1.820053 ± 0.000253	211.795955 ± 0.001304	5.0	8.0
0211615175	E2_0360	19 00 48.60	4 24 02.2	15.6	13.5	2.096534 ± 0.000089	211.563085 ± 0.000449	4.6	5.8

Table 11. continued.

CoRoTid	Winid	Right ascension (J2000.0)	Declination (J2000.0)	B	R	Period(d)	Epoch (HJD-2 454 000)	Length (h)	Depth (%)
0211617314	E1_2852	19 01 02.69	2 36 28.8	17.2	15.6	0.911478 ± 0.000072	205.506579 ± 0.001182	2.98	23.1
0211621547	E1_4182	19 01 28.51	2 44 14.5	17.4	15.9	0.912105 ± 0.000209	205.494646 ± 0.003139	6.92	0.7
0211624598	E1_3920	19 01 45.29	2 36 05.4	16.8	15.6	0.300116 ± 0.000010	204.718287 ± 0.000474	2.42	2.1
0211625631	E2_2004	19 01 50.55	3 19 25.2	17.7	15.8	0.588701 ± 0.000085	210.291918 ± 0.001652	2.52	0.6
0211625827	E2_1147	19 01 51.44	3 46 11.0	19.9	15.7	0.767518 ± 0.000092	210.330034 ± 0.001299	2.71	0.7
0211626339	E1_4042	19 01 54.02	2 03 53.4	17.4	15.7	5.348202 ± 0.000375	210.012690 ± 0.000817	5.3	9.1
0211626712	E1_0509	19 01 55.96	2 30 56.0	14.3	13.6	1.300635 ± 0.000295	205.967182 ± 0.002765	3.45	0.1
0211627602	E1_2214	19 02 00.41	3 00 38.6	17.3	14.5	0.316722 ± 0.000014	204.720023 ± 0.000636	2.04	2.0
0211627663	E1_3415	19 02 00.69	2 01 47.8	18.1	14.9	0.729238 ± 0.000116	204.85213 ± 0.001172	5.8	3.8
0211627765	E1_1819	19 02 01.19	2 28 02.4	16.2	14.6	11.868395 ± 0.004170	213.09850 ± 0.002028	4.41	3.1
0211628946	E1_2209	19 02 07.06	2 07 27.5	16.1	14.8	0.44020 ± 0.00026	204.318 ± 0.005021	4.3	26.5
0211629165	E2_0820	19 02 08.11	3 23 13.6	17.4	14.7	0.654372 ± 0.000054	210.238676 ± 0.000904	3.07	24.3
0211630757	E2_0347	19 02 15.93	3 44 23.8	15.4	13.7	1.045283 ± 0.000197	210.581559 ± 0.002095	9.7	0.3
0211631595	E1_1067	19 02 20.10	2 39 45.1	15.9	14.1	0.364522 ± 0.000018	204.9820 ± 0.00728	2.3	0.7
0211632006	E1_2962	19 02 21.88	2 34 44.4	18.3	15.8	3.690403 ± 0.000276	207.261854 ± 0.001059	7.3	11.9
0211633990	E2_0967	19 02 30.87	4 20 29.1	18.1	15.2	2.120439 ± 0.000111	211.554949 ± 0.000544	6.9	13.3
0211635934	E1_3313	19 02 39.24	2 19 38.5	16.4	15.5	0.792965 ± 0.000043	205.198137 ± 0.000703	4.00	18.4
0211636100	E2_2217	19 02 39.94	3 33 35.1	17.4	15.6	2.914761 ± 0.001650	212.478010 ± 0.005503	10.6	1.0
0211636152	E2_0448	19 02 40.16	3 38 01.0	16.2	14.2	6.538900 ± 0.001944	214.140714 ± 0.002391	15.	23.1
0211636501	E1_1776	19 02 41.66	2 17 34.5	15.4	14.3	1.139109 ± 0.000049	205.588695 ± 0.000587	3.7	4.6
0211636945	E1_3434	19 02 43.38	3 06 27.4	17.8	15.8	1.856233 ± 0.000162	204.444173 ± 0.001174	5.8	6.0
0211637024	E2_0350	19 02 43.67	3 29 56.8	14.0	13.3	7.465368 ± 0.000448	216.157339 ± 0.000393	6.5	20.4
0211639312	E1_4714	19 02 53.18	2 59 13.6	17.6	15.6	1.648806 ± 0.000091	205.628492 ± 0.000696	4.7	2.9
0211639899	E2_2283	19 02 55.54	3 33 54.4	20.0	15.9	1.087407 ± 0.000162	210.824808 ± 0.001599	6.46	0.9
0211640511	E1_4190	19 02 57.88	2 39 30.9	17.7	15.3	1.134899 ± 0.000150	205.608926 ± 0.001802	2.95	0.4
0211640538	E2_0168	19 02 57.97	3 42 54.1	14.9	12.7	5.704333 ± 0.002525	214.871488 ± 0.004016	19.4	40.
0211640753	E1_2128	19 02 58.79	2 39 36.2	16.6	15.0	1.135522 ± 0.000035	205.605992 ± 0.000417	5.1	12.3
0211640963	E1_2745	19 02 59.57	3 07 13.6	17.0	14.8	3.151352 ± 0.000144	206.064986 ± 0.000441	5.5	13.8
0211641190	E2_1806	19 03 00.37	3 33 57.8	16.9	15.0	0.562079 ± 0.000058	210.454745 ± 0.001074	4.50	13.3
0211641629	E2_1313	19 03 01.91	3 28 37.7	17.1	15.8	0.378856 ± 0.000025	209.993440 ± 0.000748	3.5	2.4
0211642536	E2_0764	19 03 05.09	3 39 41.7	19.7	15.3	1.728227 ± 0.000249	211.507758 ± 0.001469	3.63	0.4
0211642842	E2_1493	19 03 06.19	4 12 02.3	19.2	15.8	2.655287 ± 0.000437	212.268328 ± 0.001404	3.83	1.1
0211643831	E1_0484	19 03 09.63	2 41 48.1	14.2	13.0	0.873675 ± 0.000068	205.385670 ± 0.001024	7.89	2.4
0211644329	E2_1418	19 03 11.39	3 20 21.4	18.8	14.7	5.004404 ± 0.001408	212.717709 ± 0.002043	4.6	0.6
0211644737	E2_1145	19 03 12.85	3 27 51.0	15.6	13.5	2.191117 ± 0.000171	211.241016 ± 0.000782	6.3	3.0
0211644940	E1_0434	19 03 13.63	2 47 27.7	13.9	13.0	2.379552 ± 0.000326	206.880129 ± 0.001609	2.40	0.6
0211645561	E2_1926	19 03 15.74	4 23 43.2	19.6	15.8	3.469935 ± 0.000548	212.523612 ± 0.001284	9.8	9.6
0211645738	E1_3091	19 03 16.38	2 52 58.8	16.9	15.9	9.955562 ± 0.001878	211.760312 ± 0.001953	6.11	2.6
0211645932	E2_0997	19 03 17.02	3 33 42.8	15.9	13.8	0.938518 ± 0.000163	210.365920 ± 0.001788	2.42	0.2

Table 11. continued.

CoRoTid	Winid	Right ascension (J2000.0)	Declination (J2000.0)	B	R	Period(d)	Epoch (HJD-2 454 000)	Length (h)	Depth (%)
0211646179	E1_2241	19 03 17.87	2 45 09.9	16.1	14.8	3.717279 ± 0.000160	208.446760 ± 0.000555	7.4	13.
0211646637	E1_3240	19 03 19.46	1 53 39.8	16.1	15.0	8.580047 ± 0.000520	209.452014 ± 0.000670	3.53	8.6
0211646654	E1_1649	19 03 19.52	3 04 02.5	17.1	15.4	3.315650 ± 0.000418	207.078213 ± 0.001498	12.4	2.1
0211646793	E2_1530	19 03 19.97	3 18 21.2	18.8	15.4	1.895985 ± 0.000452	211.071140 ± 0.002645	5.54	1.2
0211647526	E1_2746	19 03 22.39	2 23 57.9	16.2	15.4	4.603201 ± 0.000315	207.151560 ± 0.001090	4.0	2.8
0211648306	E2_2155	19 03 24.98	3 27 53.1	17.0	15.7	1.656085 ± 0.000083	210.935940 ± 0.000542	2.66	2.8
0211649858	E2_2148	19 03 30.37	3 24 58.9	17.6	15.7	0.702002 ± 0.000103	210.223991 ± 0.001681	7.3	0.4
0211649934	E2_1548	19 03 30.62	3 26 12.2	16.5	14.3	0.616731 ± 0.000036	210.208594 ± 0.000725	2.2	12.1
0211649961	E2_2035	19 03 30.71	3 26 30.1	19.3	15.3	0.616426 ± 0.000090	210.211240 ± 0.001636	2.70	0.4
0211650128	E1_2090	19 03 31.29	2 55 33.2	15.6	14.7	0.276014 ± 0.000011	204.697371 ± 0.000552	2.38	0.5
0211650849	E1_1216	19 03 33.71	2 54 35.4	15.0	13.8	1.614741 ± 0.000062	206.161388 ± 0.000538	5.0	6.2
0211650882	E1_2180	19 03 33.81	2 35 01.4	16.1	14.9	0.756829 ± 0.000104	205.090241 ± 0.001974	3.94	0.2
0211652528	E2_1667	19 03 39.35	4 05 42.0	17.5	15.2	3.575876 ± 0.000165	212.601280 ± 0.000542	3.3	11.2
0211652558	E1_2046	19 03 39.43	2 41 32.9	15.5	13.3	0.642413 ± 0.000095	205.113285 ± 0.002018	2.60	0.4
0211652612	E1_3579	19 03 39.62	2 47 01.7	18.5	15.5	2.389667 ± 0.000210	206.326919 ± 0.001143	3.29	1.1
0211652851	E1_0744	19 03 40.33	2 41 22.6	16.3	13.6	0.641868 ± 0.000516	204.484020 ± 0.005072	2.7	0.14
0211654447	E1_1165	19 03 45.44	3 09 22.2	16.1	14.2	4.751978 ± 0.000916	208.123196 ± 0.002136	11.2	1.0
0211654657	E2_0765	19 03 46.08	3 18 44.1	15.9	14.2	1.478355 ± 0.000520	211.285937 ± 0.003505	3.62	0.1
0211655052	E1_2373	19 03 47.38	1 56 01.0	15.6	14.7	5.622826 ± 0.000372	208.061178 ± 0.000618	5.8	7.0
0211656302	E1_4561	19 03 51.30	2 45 46.6	18.1	15.7	0.795905 ± 0.000069	205.051852 ± 0.001279	7.4	2.5
0211656942	E2_0774	19 03 53.30	3 25 34.2	15.9	15.1	0.321084 ± 0.000016	209.947912 ± 0.000567	2.1	1.5
0211657070	E2_1388	19 03 53.76	3 22 38.7	15.9	14.5	6.306871 ± 0.001114	213.421628 ± 0.000820	8.6	18.4
0211657807	E1_0198	19 03 55.99	2 43 17.3	13.4	12.3	2.246592 ± 0.000085	205.84696 ± 0.000721	6.4	7.0
0211658077	E1_1339	19 03 56.83	2 21 17.8	18.6	14.6	0.781422 ± 0.000062	205.089926 ± 0.001161	3.74	0.3
0211659001	E2_1609	19 03 59.59	3 20 07.0	17.1	15.3	5.270237 ± 0.003424	215.395855 ± 0.002933	15.8	18.
0211659275	E1_1755	19 04 00.37	2 45 25.4	15.6	14.6	1.133623 ± 0.000237	205.579408 ± 0.002954	10.90	0.3
0211660194	E2_1143	19 04 03.11	3 59 41.6	17.3	15.1	2.105027 ± 0.000148	211.858954 ± 0.000665	7.1	7.5
0211660319	E1_4303	19 04 03.42	2 51 15.4	17.8	15.0	2.625383 ± 0.000181	206.116080 ± 0.000925	4.8	2.2
0211662162	E1_1012	19 04 08.94	2 25 14.1	15.6	14.7	0.308173 ± 0.000023	204.769590 ± 0.000963	3.1	3.8
0211662188	E2_1795	19 04 09.02	3 43 44.1	18.3	15.6	1.257433 ± 0.000070	211.041324 ± 0.000488	5.0	16.2
0211662385	E2_2298	19 04 09.57	3 33 26.6	17.6	15.1	0.511705 ± 0.000037	210.156281 ± 0.000829	1.99	6.6
0211663430	E2_0490	19 04 12.61	3 32 47.4	14.8	13.7	0.540217 ± 0.000062	210.300100 ± 0.001287	3.06	9.5
0211663435	E1_1548	19 04 12.63	2 12 04.7	15.5	14.7	3.319224 ± 0.000241	207.327109 ± 0.000820	7.0	6.0
0211663483	E1_2743	19 04 12.74	1 57 15.4	16.0	15.0	0.475241 ± 0.000041	204.315159 ± 0.001107	4.1	14.3
0211663717	E1_1827	19 04 13.40	3 03 35.6	15.4	14.7	8.058723 ± 0.002287	210.997104 ± 0.004020	10.1	3.0
0211663851	E1_3012	19 04 13.75	2 44 24.7	17.0	15.2	5.751727 ± 0.001381	208.884022 ± 0.002032	15.6	28.5
0211604672	E2_0436	18 59 27.30	3 32 04.1	15.2	13.3	single eclipse	228.9740 ± 0.050	12.	5.1
0211610084	E1_0947	19 00 11.37	2 32 33.9	15.7	14.1	single eclipse	209.7810 ± 0.050	7.2	7.1
0211621739	E1_0822	19 01 29.59	2 55 28.7	15.2	13.8	single eclipse	210.0865 ± 0.050	5.8	16.
0211625500	E1_1759	19 01 49.88	2 23 51.9	16.4	15.2	single eclipse	209.0106 ± 0.050	7.4	9.
0211634800	E1_3108	19 02 34.51	2 49 42.9	16.2	15.2	single eclipse	216.0102 ± 0.050	8.5	16.
0211644445	E1_3501	19 03 11.76	2 38 20.3	17.4	15.2	single eclipse	213.4666 ± 0.050	6.1	8.3

Table 11. continued.

CoRoTid	Winid	Right ascension (J2000.0)	Declination (J2000.0)	B	R	Period(d)	Epoch (HJD-2 454 000)	Length (h)	Depth (%)
0211653824	E1_0589	19 03 43.41	2 07 54.2	14.6	14.0	single eclipse	222.0337 ± 0.050	9.7	27.
0211654775	E2_0275	19 03 46.43	3 17 51.5	14.9	12.6	single eclipse	218.6824 ± 0.050	12.	4.1
0211663524	E1_4552	19 04 12.87	3 03 55.4	17.3	15.8	single eclipse	220.8275 ± 0.050	15.	12.
0211625668	E2_1728	19 01 50.74	3 18 29.8	17.8	15.8	1.771922 ± 0.000146	210.434930 ± 0.000823	3.2	7.1
						5.257641 ± 0.000685	207.316547 ± 0.001111	3.1	2.0
0211649707	E1_0564	19 03 29.91	2 33 39.4	14.8	13.2	2.118903 ± 0.000113	206.814482 ± 0.000718	1.2	4.1
0211659387	E2_1760	19 04 00.70	3 30 31.4	18.5	15.9	4.0028 ± 0.00010	212.7428 ± 0.0023	12.7	12.3
0211661262	E1_3171	19 04 06.16	2 38 50.5	18.4	14.9	18.350 ± 0.001	206.79 ± 0.01	9.5	0.7
0211603694	E1_1193	18 59 19.22	2 52 45.5	17.3	14.7	17.94 ± 0.01	208.87 ± 0.01	25.9	24.2
0211610056	E1_0447	19 00 11.16	2 56 08.3	16.6	14.1	0.39106 ± 0.000069	204.9669 ± 0.0027	3.6	2.1
0211610677	E2_1350	19 00 15.78	3 24 18.0	19.4	15.8	3.8061 ± 0.0021	213.0953 ± 0.0049	3.1	1.0
0211644461	E1_2273	19 03 11.82	2 55 38.7	16.7	14.9	15.8651 ± 0.0086	208.9181 ± 0.0051	10.3	1.1
0211646571	E1_2695	19 03 19.28	1 54 12.4	16.8	15.0	9.40426 ± 0.00776	208.4973 ± 0.0011	61.4	2.3
0211662673	E1_0836	19 04 10.43	2 29 04.0	16.4	14.2	single eclipse	209.48 ± 0.01	64.	6.5
0211605493	E1_2536	18 59 34.16	3 00 49.8	17.7	15.0	18.90985 ± 0.00323	207.2481 ± 0.0025	9.4	3.9
0211660950	E2_2115	19 04 05.23	3 52 48.8	17.8	15.6	12.87952 ± 0.00132	214.03826 ± 0.00099	7.7	14.
0211675323	E1_3431	19 04 43.07	2 24 33.0	16.3	14.6	0.961108 ± 0.000624	210.261153 ± 0.007841	1.15	0.1
0211622867	E1_2724	19 01 35.92	2 58 10.6	17.4	15.7	12.82482 ± 0.020016	211.048065 ± 0.004686	3.32	0.3
0211609212	E1_3927	19 00 04.47	3 03 12.8	18.5	15.8	2.908460 ± 0.008168	211.048894 ± 0.031810	2.80	0.3
0211639829	E1_0435	19 02 55.26	2 10 37.6	13.6	13.2	1.233351 ± 0.000747	209.951218 ± 0.007228	0.60	0.7

high priority candidates. Nevertheless, until now, none of them have been confirmed as a planet. For seven of the candidates, the detected signal could be attributed to a stellar origin, but the nature of the remaining candidates needs to be investigated further with future observations. In particular, eight priority 1 and 2 cases in the field remain good planetary candidates. The large observational effort needed to determine the nature of the CoRoT transit candidates was highlighted already in previous publications (see e.g. Moutou et al. 2009). An additional complicating factor for the SRc01 data is that the short duration of the observations (26 days) causes less accurately determined transit parameters than the previously observed CoRoT fields, thereby making subsequent follow-up observations more challenging. This is particulary so when the follow-up is not performed in the same season as the CoRoT observations.

The detection statistics of the CoRoT observations can be used as a performance estimate as outlined in Aigrain et al. (2009); Cabrera et al. (2009); Carpano et al. (2009); Moutou et al. (2009). Figure 6 shows the R magnitude versus the transit signal (the product of the transit depth and the square root of the number of in-transit measurements, as described in Pont et al. 2006) for all the objects described in this paper. The CoRoT planets considered include CoRoT-1b (Barge et al. 2008a); CoRoT-2b (Alonso et al. 2008; Bouchy et al. 2008); CoRoT-4b (Aigrain et al. 2008; Moutou et al. 2008); CoRoT-5b (Rauer et al. 2009); CoRoT-6b (Fridlund et al. 2010); CoRoT-7b (Léger et al. 2009; Queloz et al. 2009); CoRoT-8b (Bordé et al. 2010); CoRoT-9b (Deeg et al. 2010); CoRoT-10b (Bonomo et al. 2010); CoRoT-11b (Gandolfi et al. 2010); CoRoT-12b (Gillon et al. 2010); CoRoT-13b (Cabrera et al. 2010); CoRoT-14b (Tingley et al. 2011); CoRoT-16b (Ollivier, in prep.); CoRoT-17b (Csizmadia et al. 2011); CoRoT-18b (Hébrard et al. 2011); CoRoT-19b (Guenther et al. 2012); CoRoT-20b (Deleuil et al. 2012); CoRoT-21b (Paetzold, in prep.); CoRoT-22b (Moutou et al., in prep.); CoRoT-23b (Rouan et al. 2012); CoRoT-24b and c (Alonso et al., in prep.), and as well as two brown-dwarfs CoRoT-3b (Deleuil et al. 2008); and CoRoT-15b (Bouchy et al. 2011). We see a similar trend to the one found in IRa01 (Moutou et al. 2009) and LRc01 (Cabrera et al. 2009): Jupiter and Neptune-sized planets are within the photometric reach of CoRoT over the whole magnitude range, whereas small, terrestrial-sized planets are only reachable at the bright end. If we compare the depths of the detections in both runs (see Fig. 7), LRc01 performs slightly better than SRc01, an expected result, since the length of the observations (145 days instead of 26) allows one to integrate more transits and achieve a higher signal-to-noise ratio. Another expected difference is shown in Fig. 8, which compares the depth of the detections as a function of period; this figure implies that the detection limit is not reached for periods longer than three days. In LRc01, the limiting period was around ten days.

It is clear that the absolute number of detections (eclipsing binaries and planetary candidates) is not very different in both runs: 187 in SRc01 and 200 in LRc01. According to the discussion in Cabrera et al. (2009), we expect around a 50% relative detection yield in a 26 day run when compared to a long run; however, we find 90% while observing only 60% of the targets (6974 in SRc01 and 11408 in LRc01). We understand that this difference is caused by the different stellar populations observed. Although the SRc01 and the LRc01 fields are separated by only a few degrees in the sky, the stellar populations observed are very different (65% dwarf stars in SRc01 and 42% in LRc01). On the other hand, the extinction in the regions close to the plane of the Galaxy can be very inhomogeneous from one pointing to the next (see, for example, Schlegel et al. 1998). The shape of the color–magnitude diagrams of both runs suggests that the fields have different extinction rates and therefore study different parts of the Galaxy, although the impact of this effect is not fully understood. A more detailed study of the CoRoT detection statistics, taking more observed fields into account is ongoing, and will be the subject of a forthcoming paper.

Acknowledgements. The team at IAC acknowledges support by grant ESP2007-65480-C02-02 of the Spanish Ministerio de Ciencia e Inovación. The German CoRoT Team (TLS and the University of Cologne) acknowledges DLR grants 50OW0204, 50OW0603 and 50QM1004. Some of the data published in this article were acquired with the IAC80 telescope operated by the Instituto de Astrofísica de Canarias in the Observatorio del Teide, and special thanks is given to its staff for performing a large fraction of these observations. This research has made use of the Exo-Dat database, operated at LAM-OAMP, Marseille, France, on behalf of the CoRoT/Exoplanet program, whose input catalogue was made possible thanks to observations collected for years at the Isaac Newton Telescope (INT), operated on the island of La Palma by the Isaac Newton group in the Spanish Observatorio del Roque de Los Muchachos of the Instituto de Astrofísica de Canarias. This publication made use of NASA's Astrophysics Data System Bibliographic Services and of data products from the Two Micron All Sky Survey, which is a joint project of the University of Massachusetts and the Infrared Processing and Analysis Center/California Institute of Technology, funded by the National Aeronautics and Space Administration and the National Science Foundation.

References

Aigrain, S., Collier Cameron, A., Ollivier, M., et al. 2008, A&A, 488, L43
Aigrain, S., Pont, F., Fressin, F., et al. 2009, A&A, 506, 425
Alapini, A., & Aigrain, S. 2008, in IAU Symp. 249, ed. Y.-S. Sun, S. Ferraz-Mello, & J.-L. Zhou, 89
Alecian, G., Gebran, M., Auvergne, M., et al. 2009, A&A, 506, 69
Almenara, J. M., Deeg, H. J., Aigrain, S., et al. 2009, A&A, 506, 337
Alonso, R., Auvergne, M., Baglin, A., et al. 2008, A&A, 482, L21
Appourchaux, T., Michel, E., Auvergne, M., et al. 2008, A&A, 488, 705
Auvergne, M., Bodin, P., Boisnard, L., et al. 2009, A&A, 506, 411
Baglin, A., Auvergne, M., Boisnard, L., et al. 2006, in COSPAR, Plenary Meeting, Vol. 36, 36th COSPAR Scientific Assembly, 3749
Baranne, A., Queloz, D., Mayor, M., et al. 1996, A&AS, 119, 373
Barban, C., Deheuvels, S., Baudin, F., et al. 2009, A&A, 506, 51
Barge, P., Baglin, A., Auvergne, M., et al. 2008a, A&A, 482, L17
Barge, P., Baglin, A., Auvergne, M., & the CoRoT team 2008b, in IAU Symp., 249, 3
Batalha, N. M., Borucki, W. J., Koch, D. G., et al. 2010, ApJ, 713, L109
Baudin, F., Baglin, A., Orcesi, J.-L., et al. 2006, in ESA SP-1306, ed. M. Fridlund, A. Baglin, J. Lochard, & L. Conroy, 145
Belkacem, K., Samadi, R., Goupil, M., et al. 2009, Science, 324, 1540
Boisnard, L., & Auvergne, M. 2006, in ESA SP-1306, ed. M. Fridlund, A. Baglin, J. Lochard, & L. Conroy, 19
Bonomo, A. S., Santerne, A., Alonso, R., et al. 2010, A&A, 520, A65
Bordé, P., Fressin, F., Ollivier, M., Léger, A., & Rouan, D. 2007, in Transiting Extrapolar Planets Workshop, ed. C. Afonso, D. Weldrake, & T. Henning, ASP Conf. Ser., 366, 145
Bordé, P., Bouchy, F., Deleuil, M., et al. 2010, A&A, 520, A66
Borucki, W. J., Koch, D. G., Basri, G., et al. 2011, ApJ, 736, 19
Bouchy, F., Pont, F., Melo, C., et al. 2005, A&A, 431, 1105
Bouchy, F., Queloz, D., Deleuil, M., et al. 2008, A&A, 482, L25
Bouchy, F., Moutou, C., Queloz, D., & the CoRoT Exoplanet Science Team. 2009, in IAU Symp. 253, 129
Bouchy, F., Deleuil, M., Guillot, T., et al. 2011, A&A, 525, A68
Brown, T. M. 2003, ApJ, 593, L125
Cabrera, J., Fridlund, M., Ollivier, M., et al. 2009, A&A, 506, 501
Cabrera, J., Bruntt, H., Ollivier, M., et al. 2010, A&A, 522, A110
Carpano, S., & Fridlund, M. 2008, A&A, 485, 607
Carpano, S., Cabrera, J., Alonso, R., et al. 2009, A&A, 506, 491
Carrier, F., De Ridder, J., Baudin, F., et al. 2010, A&A, 509, A73
Chadid, M., Benkő, J. M., Szabó, R., et al. 2010, A&A, 510, A39
Charbonneau, D., Brown, T. M., Burrows, A., & Laughlin, G. 2007, Protostars and Planets V, 701
Charpinet, S., Green, E. M., Baglin, A., et al. 2010, A&A, 516, L6
Csizmadia, S., Moutou, C., Deleuil, M., et al. 2011, A&A, 531, A41
Damiani, C., Maceroni, C., Cardini, D., et al. 2010, Ap&SS, 328, 91

de Ridder, J., Barban, C., Baudin, F., et al. 2009, Nature, 459, 398
Debosscher, J., Sarro, L. M., López, M., et al. 2009, A&A, 506, 519
Deeg, H. J., Gillon, M., Shporer, A., et al. 2009, A&A, 506, 343
Deeg, H. J., Moutou, C., Erikson, A., et al. 2010, Nature, 464, 384
Defaÿ, C., Deleuil, M., & Barge, P. 2001, A&A, 365, 330
Degroote, P., Aerts, C., Ollivier, M., et al. 2009a, A&A, 506, 471
Degroote, P., Briquet, M., Catala, C., et al. 2009b, A&A, 506, 111
Degroote, P., Briquet, M., Auvergne, M., et al. 2010, A&A, 519, A38
Deheuvels, S., & Michel, E. 2010, Ap&SS, 328, 259
Deheuvels, S., Bruntt, H., Michel, E., et al. 2010, A&A, 515, A87
Deleuil, M., Moutou, C., Deeg, H. J., et al. 2006, in ESA SP-1306, ed. M. Fridlund, A. Baglin, J. Lochard, & L. Conroy, 341
Deleuil, M., Deeg, H. J., Alonso, R., et al. 2008, A&A, 491, 889
Deleuil, M., Meunier, J. C., Moutou, C., et al. 2009, AJ, 138, 649
Deleuil, M., Bonomo, A. S., Ferraz-Mello, S., et al. 2012, A&A, in press DOI: 10.1051/0004-6361/201117681
Desmet, M., Frémat, Y., Baudin, F., et al. 2010, MNRAS, 401, 418
Diago, P. D., Gutiérrez-Soto, J., Auvergne, M., et al. 2009, A&A, 506, 125
Dolez, N., Vauclair, S., Michel, E., et al. 2009, A&A, 506, 159
Drummond, R., Lapeyrere, V., Auvergne, M., et al. 2008, A&A, 487, 1209
Fridlund, M., Hébrard, G., Alonso, R., et al. 2010, A&A, 512, A14
Gandolfi, D., Hébrard, G., Alonso, R., et al. 2010, A&A, 524, A55
García, R. A., Régulo, C., Samadi, R., et al. 2009, A&A, 506, 41
García, R. A., Mathur, S., Salabert, D., et al. 2010, Science, 329, 1032
García Hernández, A., Moya, A., Michel, E., et al. 2009, A&A, 506, 79
Gazzano, J.-C., de Laverny, P., Deleuil, M., et al. 2010, A&A, 523, A91
Gillon, M., Hatzes, A., Csizmadia, S., et al. 2010, A&A, 520, A97
Guenther, E. W., Díaz, R. F., Gazzano, J.-C., et al. 2012, A&A, 537, A136
Gutiérrez-Soto, J., Floquet, M., Samadi, R., et al. 2009, A&A, 506, 133
Hébrard, G., Evans, T. M., Alonso, R., et al. 2011, A&A, 533, A130
Hekker, S., Kallinger, T., Baudin, F., et al. 2009, A&A, 506, 465
Hekker, S., Barban, C., Baudin, F., et al. 2010, A&A, 520, A60
Howard, A. W., Marcy, G. W., Bryson, S. T., et al. 2011, ApJ, submitted [arXiv:1103.2541]
Huat, A., Hubert, A., Baudin, F., et al. 2009, A&A, 506, 95
Lefever, K., Puls, J., Morel, T., et al. 2010, A&A, 515, A74
Léger, A., Rouan, D., Schneider, J., et al. 2009, A&A, 506, 287
Loeillet, B., Bouchy, F., Deleuil, M., et al. 2008, A&A, 479, 865
Maceroni, C., Montalbán, J., Michel, E., et al. 2009, A&A, 508, 1375
Mayor, M., Udry, S., Lovis, C., et al. 2009, A&A, 493, 639
Maceroni, C., Cardini, D., Damiani, C., et al. 2010, Astron. Nachr., in press [arXiv:1004.1525]
Mazeh, T., Guterman, P., Aigrain, S., et al. 2009, A&A, 506, 431
Meunier, J.-C., Deleuil, M., Moutou, C., Ouchani, M., Savalle, R., & Surace, C. 2007, in Astronomical Data Analysis Software and Systems XVI, ed. R. A. Shaw, F. Hill, & D. J. Bell, ASP Conf. Ser., 376, 339
Michel, E., Baglin, A., Auvergne, M., et al. 2008, Science, 322, 558
Miglio, A., Montalbán, J., Baudin, F., et al. 2009a, A&A, 503, L21
Miglio, A., Montalbán, J., Eggenberger, P., Hekker, S., & Noels, A. 2009b, in AIP Conf. Ser. 1170, ed. J. A. Guzik, & P. A. Bradley, 132
Mislis, D., Schmitt, J. H. M. M., Carone, L., Guenther, E. W., & Pätzold, M. 2010, A&A, 522, A86
Mosser, B., Michel, E., Appourchaux, T., et al. 2009, A&A, 506, 33
Mosser, B., Belkacem, K., Goupil, M., et al. 2010, A&A, 517, A22
Moutou, C., Pont, F., Barge, P., et al. 2005, A&A, 437, 355
Moutou, C., Aigrain, S., Almenara, J., et al. 2007, in Transiting Extrapolar Planets Workshop, ed. C. Afonso, D. Weldrake, & T. Henning, ASP Conf. Ser., 366, 127
Moutou, C., Bruntt, H., Guillot, T., et al. 2008, A&A, 488, L47
Moutou, C., Pont, F., Bouchy, F., et al. 2009, A&A, 506, 321
Neiner, C., Gutiérrez-Soto, J., Baudin, F., et al. 2009, A&A, 506, 143
Ofir, A., Alonso, R., Bonomo, A. S., et al. 2010, MNRAS, 404, L99
Pepe, F., Mayor, M., Galland, F., et al. 2002, A&A, 388, 632
Pinheiro da Silva, L., Rolland, G., Lapeyrere, V., & Auvergne, M. 2008, MNRAS, 384, 1337
Pont, F., Zucker, S., & Queloz, D. 2006, MNRAS, 373, 231
Poretti, E., Michel, E., Garrido, R., et al. 2009, A&A, 506, 85
Queloz, D., Bouchy, F., Moutou, C., et al. 2009, A&A, 506, 303
Rabus, M., Alonso, R., Belmonte, J. A., et al. 2009, A&A, 494, 391
Rauer, H., Queloz, D., Csizmadia, S., et al. 2009, A&A, 506, 281
Régulo, C., Almenara, J. M., Alonso, R., Deeg, H., & Roca Cortés, T. 2007, A&A, 467, 1345
Renner, S., Rauer, H., Erikson, A., et al. 2008, A&A, 492, 617
Rouan, D., Parviainen, H., Moutou, C., et al. 2012, A&A, 537, A54
Samadi, R., Ludwig, H., Belkacem, K., et al. 2010, A&A, 509, A16
Santerne, A., Endl, M., Hatzes, A., et al. 2011, in Detection and Dynamic of Transiting Exoplanets, St. Michel l'Observatoire, France, ed. F. Bouchy, R. Díaz, & C. Moutou, EPJ Web Conf., id. 02001
Sarro, L. M., Debosscher, J., Aerts, C., & López, M. 2009, A&A, 506, 535
Schlegel, D. J., Finkbeiner, D. P., & Davis, M. 1998, ApJ, 500, 525
Skrutskie, M. F., Cutri, R. M., Stiening, R., et al. 2006, AJ, 131, 1163
Tingley, B., Endl, M., Gazzano, J., et al. 2011, A&A, 528, A97
Weiss, W. W., Aerts, C., Aigrain, S., et al. 2004, in Stellar Structure and Habitable Planet Finding, ed. F. Favata, S. Aigrain, & A. Wilson, ESA Spec. Publ., 538, 435

[1] Institute of Planetary Research, German Aerospace Center, Rutherfordstrasse 2, 12489 Berlin, Germany
e-mail: anders.erikson@dlr.de
[2] Laboratoire d'Astrophysique de Marseille, CNRS & University of Provence, 38 rue Frédéric Joliot-Curie, 13388 Marseille Cedex 13, France
[3] Laboratoire d'Astronomie de Lille, Université de Lille 1, 1 impasse de l'Observatoire, 59000 Lille, France
[4] Institut de Mécanique Céleste et de Calcul des Ephémérides, UMR 8028 du CNRS, 77 avenue Denfert-Rochereau, 75014 Paris, France
[5] Department of Physics, Denys Wilkinson Building Keble Road, Oxford OX1 3RH, UK
[6] School of Physics, University of Exeter, Stocker Road, Exeter EX4 4QL, UK
[7] Instituto de Astrofísica de Canarias, 38205 La Laguna, Tenerife, Spain
[8] Observatoire de l'Université de Genève, 51 chemin des Maillettes, 1290 Sauverny, Switzerland
[9] LESIA, UMR 8109 CNRS, Observatoire de Paris, UVSQ, Université Paris-Diderot, 5 place J. Janssen, 92195 Meudon, France
[10] Universität Bern, Physics Institute, Sidlerstrasse 5, 3012 Bern, Switzerland
[11] Institut d'astrophysique spatiale, Université Paris-Sud 11 & CNRS (UMR 8617), 91405 Orsay, France
[12] Observatoire de Haute Provence, 04670 Saint Michel l'Observatoire, France
[13] Institut d'Astrophysique de Paris, UMR 7095 CNRS, Université Pierre & Marie Curie, 98bis boulevard Arago, 75014 Paris, France
[14] LUTH, Observatoire de Paris, UMR 8102 CNRS, Université Paris Diderot, 5 place Jules Janssen, 92195 Meudon, France
[15] Rheinisches Institut für Umweltforschung an der Universität zu Köln, Aachener Strasse 209, 50931 Köln, Germany
[16] Research and Scientific Support Department, ESTEC/ESA, PO Box 299, 2200 AG Noordwijk, The Netherlands
[17] University of Vienna, Institute of Astronomy, Türkenschanzstr. 17, 1180 Vienna, Austria
[18] IAG-Universidade de Sao Paulo, Brasil
[19] Thüringer Landessternwarte, Sternwarte 5, Tautenburg 5, 07778 Tautenburg, Germany
[20] Université de Nice-Sophia Antipolis, CNRS UMR 6202, Observatoire de la Côte d'Azur, BP 4229, 06304 Nice Cedex 4, France
[21] University of Liège, Allée du 6 août 17, Sart Tilman, Liège 1, Belgium
[22] Space Research Institute, Austrian Academy of Science, Schmiedlstr. 6, 8042 Graz, Austria
[23] School of Physics and Astronomy, Raymond and Beverly Sackler Faculty of Exact Sciences, Tel Aviv University, Tel Aviv, Israel
[24] Center for Astronomy and Astrophysics, TU Berlin, Hardenbergstr. 36, 10623 Berlin, Germany
[25] Dpto. de Astrofísica, Universidad de La Laguna, 38206 La Laguna, Tenerife, Spain
[26] Wise Observatory, Tel Aviv University, Tel Aviv 69978, Israel
[27] Departamento de Astronomía y Astrofísica, Pontificia Universidad Católica de Chile, Av. Vicuña Mackenna 4860, Casilla 306, Santiago 22, Chile
[28] LCOGT, 6740 Cortona Drive, Santa Barbara, CA 93117, USA
[29] Department of Physics, Broida Hall, University of California, Santa Barbara, CA 93106, USA